energy&fuels

pubs.acs.org/EF

Article

Methane Reforming with H_2S and Sulfur for Hydrogen Production: Thermodynamic Assessment

Flavio Tollini, Mattia Sponchioni, Vincenzo Calemma, and Davide Moscatelli*

Cite This: https://doi.org/10.1021/acs.energyfuels.3c01237

Read Online

ACCESS | Metrics & More | Article Recommendations | Supporting Information

ABSTRACT: Nowadays, most of the hydrogen is obtained from fossil fuels. At the same time, the effort and resources dedicated to the development of sustainable hydrogen manufacturing processes are rapidly increasing to promote the energy transition toward renewable sources. In this direction, a potential source of hydrogen could be hydrogen sulfide, produced as a byproduct in several processes, and in particular in the oil extraction and refinery operations. Methane reforming using H_2S has recently attracted much interest for its economic and environmental implications. Its conversion, in fact, provides a viable way for the elimination of a hazardous molecule, producing a high-added value product like hydrogen. At the same time, some of the still open key aspects of this process are the coke deposition due to thermal pyrolysis of methane and the process endothermicity. In this work, the methane reforming with H_2S by co-feeding sulfur is investigated through a detailed thermodynamic analysis as a way to alleviate the critical aspects highlighted for the process. A parametric analysis was conducted to assess the best thermodynamic conditions in terms of pressure, temperature, and feed composition. Changing the sulfur, H_2S, and methane feed composition can enhance the system by improving the hydrogen production yield, reducing the carbon and sulfur deposition, increasing the H_2S removal efficiency, and reducing the necessary thermal duty.

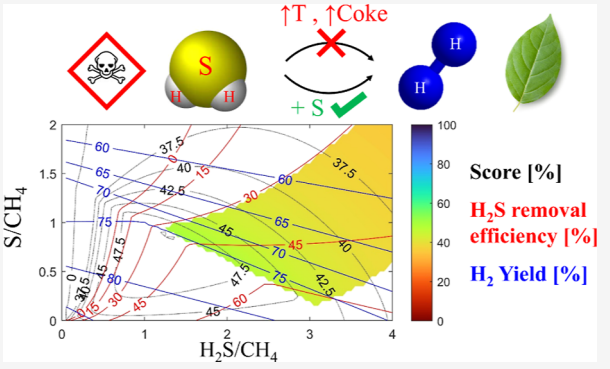

1. INTRODUCTION

Hydrogen is a large-scale commodity with a yearly production ranging from 70 to 110 Mt/y.[1,2] Currently, hydrogen is mainly used for the synthesis of ammonia (27%), methanol (11%), and in refinery processes (33%), such as in the hydrodesulfurization of fuels and hydrocracking of oil cuts.[3] To ensure this large hydrogen demand, large production plants mainly based on steam methane reforming (SMR) (49−51%), gasification of coal (CG) (23−25%), and gasification of oil (OG) (18−21%) have been installed. It is evident that these processes largely rely on the exploitation of fossil fuels. In addition, SMR, OG, and CG are associated with a wide production of greenhouse gases (GHGs), reaching up to 10−11 t_{CO2}/t_{H2} and 19 t_{CO2}/t_{H2} for SMR and CG, respectively.[4,5] Only recently, the production of hydrogen through environmentally friendly processes has become the object of intense research. Among these processes, water electrolysis is the most studied and acquires industrial maturity.[1,2] Biomass-derived hydrogen is also appealing. This can be produced with interesting efficiency from the chemical looping steam reforming of glycerol, a byproduct of the biodiesel industry, coupled with CO_2 capture.[6]

Another potential source of hydrogen not yet exploited so far is hydrogen sulfide (H_2S). Hydrogen sulfide is present in many gas wells, and a significant fraction of the known natural gas reserves have concentrations of H_2S so high that their exploitation is uneconomical. According to the International energy agency (IEA), over 40% of the world's gas reserves are sour,[7] meaning they present a significant concentration of acidic compounds such as carbon dioxide (CO_2) and hydrogen sulfide. H_2S is also produced in large quantities in the desulfurization of oil cuts. For example, a medium-sized refinery that processes 10 million tons of oil annually produces about 10 kton/y of H_2S. It is estimated that the world production of H_2S is about 80 Mt/y, out of which about 5 Mt/y of hydrogen could potentially be obtained, with a saving in CO_2 emissions of 50 Mt/y if compared to the traditional hydrogen produced via SMR.[8]

Nowadays, the conversion of H_2S, which due to its toxicity needs to be reduced below a concentration of a few ppm, is generally carried out by adsorption with amines.[9] Once separated from hydrocarbons, the process used commercially for the conversion of H_2S is the Claus process. In this process, one-third of H_2S is oxidized to SO_2, which subsequently reacts

Received: April 10, 2023
Revised: June 23, 2023

with the remaining part of H_2S to produce sulfur and water according to the scheme below.

$$H_2S + 3/2O_2 \rightarrow SO_2 + 2O \qquad \Delta H^\circ = -518 \text{ kJ mol}^{-1} \tag{r.1}$$

$$2H_2S + SO_2 \rightarrow 3/8S_8 + 2H_2O \qquad \Delta H^\circ = -107 \text{ kJ mol}^{-1} \tag{r.2}$$

In the first step, the oxidation of H_2S to water and sulfur dioxide is carried out. Then, H_2S is reacted with SO_2, yielding sulfur and water. Although the Claus process efficiently converts H_2S, it has the disadvantage of degrading hydrogen into water, thus preventing the recovery of this important energy vector. Furthermore, a problem of the Claus process is the presence of SO_2 in the exhaust gases caused by the fact that it is necessary to operate with stoichiometric excess to complete r.r.1. It is therefore necessary to post-process exhaust gases with expensive purification treatments to comply with the legal limits on SO_2 emissions.

A valuable alternative to producing hydrogen from H_2S is the exploitation of this compound for methane reforming.[10,11] In fact, this process would convert a waste feedstock into high-added value hydrogen with low environmental impact. The reforming of methane with H_2S is schematized in r.r.3[10−13]

$$2H_2S + CH_4 \rightarrow CS_2 + 4H_2 \qquad \Delta H^\circ = 232 \text{ kJ mol}^{-1} \tag{r.3}$$

When conducted under appropriate conditions, the methane reforming using H_2S (H_2SMR), r.r.3, yields molecular hydrogen, while sulfur is present in the products as carbon disulfide (CS_2). El-Melih et al.[13,14] investigated the effect of temperature and residence time on H_2S splitting and H_2S reformation in the presence of methane under homogeneous conditions. The experiments were conducted in a plug-flow reactor selecting appropriate conditions to avoid carbon formation. It was found that the presence of methane increased H_2S conversion, and 95% H_2 recovery was achieved. Numerical and experimental tests show that the decomposition of H_2S and methane occurred both thermally and chemically. Among the reasons behind the increase in H_2S conversion caused by CH_4 is the higher concentration of H radicals in the reaction pool due to the methane decomposition at lower temperatures.

Li et al.[15,16] developed a detailed kinetic mechanism involving 85 species and 515 reactions for H_2SMR under dilute conditions. The effects of temperature and the initial H_2S/CH_4 ratio on H_2 production and conversion of H_2S and CH_4 were experimentally investigated, and the system was kinetically analyzed. The conversion of H_2S showed a steady increase with temperature, while the reactivity of CH_4 was low below 1000 °C. At higher temperatures, the conversion of CH_4 increased rapidly, leading to higher H_2 yields and the formation of CS_2. The analysis of the results provided by the kinetic model showed that the CH_4 reactivity depended on the S radical, yielding SH and CH_3 radicals. Experiments showed that the best H_2S/CH_4 ratio for H_2 production is 2 at a temperature over 1250 °C.

The thermodynamic equilibrium at high temperatures of methane and hydrogen sulfide has been investigated by Megalofonos,[17] Huang,[12,18] and, more recently, Pellegrini.[19] The main findings of these studies can be summarized as follows:

- Going from low to high temperatures, the H_2SMR process can be broadly divided into three regimes: (i) CH_4 pyrolysis (T < 800 °C); (ii) both CH_4 pyrolysis and H_2SMR (T = 800÷1200); and (iii) H_2SMR plus partial H_2S pyrolysis (T > 1200 °C).
- The threshold temperature to avoid carbon formation depends on the H_2S/CH_4 ratio. For an H_2S/CH_4 ratio of 3 or lower, it is not possible to avoid the formation of carbon, while lowering the threshold temperature down to 1000 °C is necessary for an H_2S/CH_4 molar ratio of 10.
- Increasing the reaction pressure leads to a significant increase in the threshold temperature to avoid carbon formation.
- Beyond 1000 °C, sulfur yields show a steady increase with the temperature to reach values between 80 and 30% at 2000 °C depending on the operating conditions.

Although H_2SMR allows for the recovery of the hydrogen contained in H_2S, the process presents a series of drawbacks that have so far precluded its scale-up and commercial application. On one side, r.r.3 is strongly endothermic. Consequently, a considerable amount of energy must be supplied to the system by the combustion of a fuel, with a considerable increase in operating costs.

In addition, preventing the formation of carbon is essential to avoiding rapid deactivation of the catalyst or plugging of the reactor. The thermodynamic analysis of the system[11,19] showed that the reaction must be performed at elevated temperatures to avoid carbon formation. In particular, temperatures above 1400 °C and a H_2S/CH_4 molar ratio of 4 are required. To lower this threshold temperature for the carbon formation (TTC) up to 1000 °C, a much higher H_2S/CH_4 ratio is required, which results in a significant increase in the thermal duty[19] and a notable worsening of the economics caused mainly by the decrease in the conversion per step of H_2S.[20]

In this work, an innovative approach to alleviating the limitations currently encountered in methane reforming with H_2S is presented. Specifically, methane reforming co-feeding H_2S and sulfur (S−H_2SMR) is reported for the first time. A systematic thermodynamic analysis of the process is conducted, exploring the effect of temperature, pressure, and composition of the mixture fed to the process on the equilibrium composition of the system. It was demonstrated that the presence of sulfur in the methane reforming with H_2S allows the reutilization of an additional waste feedstock from the Claus process, reduces the endothermicity of the overall process, and simultaneously reduces the TTC.

2. MATERIALS AND METHODS

This work investigates the equilibrium composition of the S−H_2SMR by changing the composition of the feed, the operative reaction temperature, and the pressure for the following set of conditions:

- $\beta = {}^{n^0_{H_2S}}/_{n^0_{CH_4}}$ inlet molar ratio of H_2S/CH_4 = 0−4;
- $\gamma = {}^{n^0_{S_2}}/_{n^0_{CH_4}}$ inlet molar ratio of S_2/CH_4 = 0−2;
- Temperature = 400−3000 °C; and
- Pressure = 0.1−20 atm.

The conversion of one species is calculated as the ratio between the molar consumption and the initial amount. For example, for CH_4 and H_2S, the conversion is calculated by eq 1, where the mol_i^{in} and mol_i^{out} are the inlet and outlet moles of the i-th compound, respectively. In this work, the conversion of H_2S will be referred to as "H_2S removal efficiency". The total sulfur conversion is calculated by eq 2,

https://doi.org/10.1021/acs.energyfuels.3c01237
Energy Fuels XXXX, XXX, XXX−XXX

considering the sulfur present in H_2S and the generic allotropic sulfur form.

$$\chi_i\ \% = \frac{\mathrm{mol}_i^{\mathrm{in}}}{mol_i^{in}} \times 100 \tag{1}$$

$$\chi_S\ \% = \frac{\left(\sum n\ \mathrm{mol}_{S_n}^{\mathrm{in}} + \mathrm{mol}_{H_2S}^{\mathrm{in}}\right) - \left(\sum n\ \mathrm{mol}_{S_n}^{\mathrm{out}} + \mathrm{mol}_{H_2S}^{\mathrm{out}}\right)}{\left(\sum n\ \mathrm{mol}_{S_n}^{\mathrm{in}} + \mathrm{mol}_{H_2S}^{\mathrm{in}}\right)} \times 100 \tag{2}$$

The H_2 and CS_2 selectivity (σ_i) are calculated in eqs 3 and 4 as the ratio between the produced moles of the i-th compound of interest and the molar consumption of all the possible sources.

$$\sigma_{H_2}\ \% = \frac{\mathrm{mol}_{H_2}^{\mathrm{out}}}{(2\ \mathrm{mol}_{CH_4}^{\mathrm{in}} + \mathrm{mol}_{H_2S}^{\mathrm{in}}) - (2\ \mathrm{mol}_{CH_4}^{\mathrm{out}} + \mathrm{mol}_{H_2S}^{\mathrm{out}})} \times 100 \tag{3}$$

$$\sigma_{CS_2}\ \% = \frac{\mathrm{mol}_{CS_2}^{\mathrm{out}} - \mathrm{mol}_{CS_2}^{\mathrm{in}}}{\mathrm{mol}_{CH_4}^{\mathrm{in}} - \mathrm{mol}_{CH_4}^{\mathrm{out}}} \times 100 \tag{4}$$

The H_2 and CS_2 yields (μ_i) are calculated by eqs 5 and 6 as the ratio between the produced moles of the compound i-th and the maximum obtainable from the starting mixture.

$$\mu_{H_2}\ \% = \frac{\mathrm{mol}_{H_2}^{\mathrm{out}}}{2\ \mathrm{mol}_{CH_4}^{\mathrm{in}} + \mathrm{mol}_{H_2S}^{\mathrm{in}}} \times 100 \tag{5}$$

$$\mu_{CS_2}\ \% = \frac{\mathrm{mol}_{CS_2}^{\mathrm{out}}}{\mathrm{mol}_{CH_4}^{\mathrm{in}}} \times 100 \tag{6}$$

The carbon coke and the sulfur produced (∂_i) are calculated by eqs 7 and 8 as the ratio between the produced moles of the i-th compound with respect to the maximum obtainable from the starting mixture.

$$\partial_{\mathrm{Coke}}\ \% = \frac{\mathrm{mol}_{\mathrm{Coke}}^{\mathrm{out}}}{\mathrm{mol}_{CH_4}^{\mathrm{in}}} \times 100 \tag{7}$$

$$\partial_{\mathrm{Sulfur}}\ \% = \frac{\sum n\ \mathrm{mol}_{S_n}^{\mathrm{out}} - \sum n\ \mathrm{mol}_{S_n}^{\mathrm{in}}}{\left(\sum n\ \mathrm{mol}_{S_n}^{\mathrm{in}} + \mathrm{mol}_{H_2S}^{\mathrm{in}}\right)} \times 100 \tag{8}$$

The necessary reaction heat (q) for the system is computed from the energy balance of the system, neglecting the enthalpy of mixing, as in eq 9.

$$q\left[\frac{\mathrm{kJ}}{\mathrm{mol}_{\mathrm{CH4}}^{\mathrm{Reforming}}}\right] = \left(\sum_{i=1}^{\mathrm{NC}} \mathrm{mol}_i^{\mathrm{out}} h_i(T) - \sum_{i=1}^{\mathrm{NC}} \mathrm{mol}_i^{\mathrm{in}} h_i(T)\right) / \mathrm{mol}_{\mathrm{CH4}}^{\mathrm{in}} \tag{9}$$

Assuming the methane heat of combustion $\Delta H_{\mathrm{CH4}}^{\mathrm{comb}}$ = 890.7 kJ/$\mathrm{mol}_{\mathrm{CH4}}^{\mathrm{burned}}$, it is possible to estimate the percentage of equivalent methane burned to heat the system with respect to the total amount of consumed methane (reformed + burned) by eq 10.

$$\mathrm{CH}_4^{\mathrm{burned}}\ \% = \frac{q/\Delta H_{\mathrm{CH4}}^{\mathrm{comb}}}{1 + q/\Delta H_{\mathrm{CH4}}^{\mathrm{comb}}} \times 100 \tag{10}$$

All the thermodynamic parameters used in this work were obtained from the NIST Webbook[21] and Perry's Handbook.[22] The heat capacity $C_{p,i}^0(T)$, enthalpy of formation $h_{f,i}^0(T)$, entropy of formation $s_{f,i}^0(T)$, and Gibbs free energy of formation $g_{f,i}^0(T)$ are calculated based on the Shomate equations[23] reported in eqs S1–S4. The enthalpy $\Delta h_{R,j}^0(T)$, entropy $\Delta s_{R,j}^0(T)$, and Gibbs free energy $\Delta g_{R,j}^0(T)$ of the reaction are calculated based on eqs S5–S7. The number of independent reactions (NR) necessary to characterize the equilibrium state is computed as the difference between the number of species (NC) and the rank of the matrix atom-species (**A**) (NR = NC − rank(**A**)). Defining the extent of the generic reaction j as λ_j, it is possible to evaluate the number of moles of the species i at the equilibrium state ($\mathrm{mol}_i^{\mathrm{out}}$) knowing the initial moles of the i-th component ($\mathrm{mol}_i^{\mathrm{in}}$) according to eq S8.

By exploiting the Soave–Redlich–Kwong (SRK) equation of state (EoS), it is possible to calculate the activity $a_i(T,P,\mathrm{Pref},\lambda_1, ...,\lambda_{\mathrm{NR}})$ of the i-th species depending on temperature, pressure, and the extent of all the reactions.

With this approach, the original problem with NC unknowns can be rewritten with only NR unknowns.

To calculate the NR extent of reactions λ_j, it is necessary to solve the non-linear system composed of the NR equilibrium equations for the NR independent reactions obtained from eq 11, where R is the universal gas constant.

$$K_{\mathrm{eq,j}} = \prod_{i=1}^{\mathrm{NC}} a_i(T,\ P,\ \mathrm{Pref},\ \lambda_1,\ ...,\ \lambda_{\mathrm{NR}})^{\nu_{i,j}} = \exp\left(-\frac{\Delta G_{\mathrm{R,j}}^0(T)}{R\ T}\right) \tag{11}$$

The solution of this non-linear system was computed in Matlab with the *genetic algorithm (GA)* solver, comparing the results with the simulations performed in a Gibbs reactor in Aspen HYSYS. The atom material balance was calculated for all the simulations to assess the reliability of the numerical solution.

To characterize the equilibrium, it is necessary to define which species are interested in being studied and, subsequently, the reaction involved. For this reason, it is possible to distinguish three situations (see Table 1):

Table 1. Species Considered for the Equilibrium Characterization

simplified pure-methane reforming sulfur-based	simplified mixed-methane reforming	mixed-methane reforming
S_2, CH_4, CS_2, CS, H_2S, C, H_2	S_2, O_2, CO_2, CO, H_2O, SO_2, SO_3, CH_4, CS_2, CS, H_2S, C, H_2	S, S_2, S_3, S_4, S_5, S_6, S_7, S_8, O_2, CO_2, CO, H_2O, SO_2, SO_3, CH_4, CS_2, CS, H_2S, C, H_2

1) Methane reforming with sulfur, negligible oxygenated compounds, and allotropic sulfur lumping.

Under these conditions, it is possible to maximize the productivity of H_2, reducing the CO_x and SO_x emissions to zero due to side reactions. This situation can be performed with dry gaseous streams without CO_x.

2) Methane reforming with sulfur and non-negligible oxygenated compounds.

The system becomes more complex if the gaseous streams used for the sulfur–methane reforming contain traces of oxygenated molecules such as water or CO_x. Under these conditions, the oxygenated compounds are more thermodynamically stable than the sulfur compounds (see Figure S1 and Table S1). These thermodynamic properties drastically reduce the reaction selectivity and yield.

3) Methane reforming with sulfur, non-negligible oxygenated compounds, and different sulfur allotropic forms.

This case study is the most complete but, at the same time, the most computationally demanding. To consider the different sulfur allotropic forms, the total number of species increases from 13 (case 2) to 20 (with S_x x = 1,...,8), and the necessary reactions to characterize the equilibrium conditions increase to NR = 16.

This work deeply studied the first proposed case for combined H_2S-methane reforming enhanced by sulfur methane oxidation.

https://doi.org/10.1021/acs.energyfuels.3c01237
Energy Fuels XXXX, XXX, XXX−XXX

Table 2. Enthalpy of Reaction $\Delta H^0_{R,j}$, Entropy of Reaction $\Delta S^0_{R,j}$, Gibbs Free Energy of Reaction $\Delta G^0_{R,j}$, and Equilibrium Constant K_{eq} for Oxygen-Based (R^O_j) and Sulfur-Based (R^S_j) Reactions at 25 °C and 1 atm

	reaction	$\Delta H_R°$ [kJ mol^{-1}]	$\Delta S_R°$ [J mol^{-1}K^{-1}]	$\Delta G_R°$ [kJ mol^{-1}]	K_{eq} [−]
	Reaction 1: Partial Methane Reforming				
R^O_1	$CH_{4(g)} + H_2O_{(g)} \leftrightarrow CO_{(g)} + 3H_{2(g)}$	206.17	214.61	142.18	1.23×10^{-25}
R^S_1	$CH_{4(g)} + H_2S_{(g)} \leftrightarrow CS_{(g)} + 3H_{2(g)}$	375.80	210.57	313.01	1.44×10^{-55}
	Reaction 2: Complete Methane Reforming				
R^O_2	$CH_{4(g)} + 2H_2O_{(g)} \leftrightarrow CO_{2(g)} + 4H_{2(g)}$	165.01	172.58	113.56	1.27×10^{-20}
R^S_2	$CH_{4(g)} + 2H_2S_{(g)} \leftrightarrow CS_{2(g)} + 4H_{2(g)}$	232.99	162.91	184.43	4.87×10^{-33}
	Reaction 3: Partial Coke Reforming				
R^O_3	$C_{(s)} + H_2O_{(g)} \leftrightarrow CO_{(g)} + H_{2(g)}$	128.12	133.5	88.315	3.37×10^{-16}
R^S_3	$C_{(s)} + H_2S_{(g)} \leftrightarrow CS_{(g)} + H_{2(g)}$	297.74	129.46	259.14	3.96×10^{-46}
	Reaction 4: Complete Coke Reforming				
R^O_4	$C_{(s)} + 2H_2O_{(g)} \leftrightarrow CO_{2(g)} + 2H_{2(g)}$	86.96	81.47	59.69	3.49×10^{-11}
R^S_4	$C_{(s)} + 2H_2S_{(g)} \leftrightarrow CS_{2(g)} + 2H_{2(g)}$	154.95	91.79	130.56	1.33×10^{-23}
	Reaction 5: Water/H_2S Gas Shift				
R^O_5	$CO_{(g)} + H_2O_{(g)} \leftrightarrow CO_{2(g)} + H_{2(g)}$	−41.16	−42.03	−28.63	1.04×10^{5}
R^S_5	$CS_{(g)} + H_2S_{(g)} \leftrightarrow CS_{2(g)} + H_{2(g)}$	−142.80	−47.67	−128.59	3.38×10^{22}
	Reaction 6: Partial Methane Oxidation 1				
R^O_6	$CH_{4(g)} + {}^1/_2O_{2(g)} \leftrightarrow CO_{(g)} + 2\,H_{2(g)}$	−35.66	170.19	−86.40	1.37×10^{15}
R^S_6	$CH_{4(g)} + {}^1/_2S_{2(g)} \leftrightarrow CS_{(g)} + 2\,H_{2(g)}$	290.9	171.56	239.75	9.91×10^{-43}
	Reaction 7: Partial Methane Oxidation 2				
R^O_7	$CH_{4(g)} + O_{2(g)} \leftrightarrow CO_{2(g)} + 2H_{2(g)}$	−318.64	83.75	−343.61	1.59×10^{-60}
R^S_7	$CH_{4(g)} + S_{2(g)} \leftrightarrow CS_{2(g)} + 2H_{2(g)}$	63.21	84.89	37.90	2.29×10^{-7}
	Reaction 8: Partial Methane Oxidation 3				
R^O_8	$CH_{4(g)} + {}^3/_2\,O_{2(g)} \leftrightarrow CO_{(g)} + 2\,H_2O_{(g)}$	−519.32	81.36	−543.57	1.72×10^{95}
R^S_8	$CH_{4(g)} + {}^3/_2\,S_{2(g)} \leftrightarrow CS_{(g)} + 2H_2S_{(g)}$	121.1	93.55	93.21	4.67×10^{-17}
	Reaction 9: Complete Methane Oxidation				
R^O_9	$CH_{4(g)} + 2O_{2(g)} \leftrightarrow CO_{2(g)} + 2H_2O_{(g)}$	−802.30	−5.09	−800.78	1.99×10^{140}
R^S_9	$CH_{4(g)} + 2S_{2(g)} \leftrightarrow CS_{2(g)} + 2H_2S_{(g)}$	−106.59	6.87	−108.64	1.08×10^{19}
	Reaction 10: Partial Coke Oxidation				
R^O_{10}	$C_{(s)} + {}^1/_2O_{2(g)} \leftrightarrow CO_{(g)}$	−113.71	89.08	−140.27	3.77×10^{24}
R^S_{10}	$C_{(s)} + {}^1/_2\,S_{2(g)} \leftrightarrow CS_{(g)}$	212.84	90.45	185.88	2.72×10^{-33}
	Reaction 11: Complete Coke Oxidation				
R^O_{11}	$C_{(s)} + O_{2(g)} \leftrightarrow CO_{2(g)}$	−396.70	2.64	−397.48	4.36×10^{69}
R^S_{11}	$C_{(s)} + S_{2(g)} \leftrightarrow CS_{2(g)}$	−14.85	3.78	−15.98	6.29×10^{2}
	Reaction 12: Water/H_2S Decomposition				
R^O_{12}	$H_2O_{(g)} \leftrightarrow H_{2(g)} + {}^1/_2\,O_{2(g)}$	241.83	44.42	228.59	8.94×10^{-41}
R^S_{12}	$H_2S_{(g)} \leftrightarrow H_{2(g)} + {}^1/_2\,S_{2(g)}$	84.90	39.01	73.27	1.46×10^{-13}
	Reaction 13: Methane Decomposition				
R_{13}	$CH_{4(g)} \leftrightarrow C_{(s)} + 2H_{2(g)}$	78.05	81.11	53.87	3.65×10^{-10}

3. RESULTS AND DISCUSSION

3.1. Methane Reforming: Oxygen vs Sulfur-Based Process. In Figures S1 and S2, the calculated enthalpy $h^0_{f,i}(T)$, entropy $s^0_{f,i}(T)$, and Gibbs free energy $g^0_{f,i}(T)$ of formation are shown as a function of temperature for all the species reported in Table 1. All oxygen-based compounds (O_2, CO_2, CO, and H_2O) are more stable than their sulfur-based counterparts (S_2, CS_2, CS, and H_2S), having similar $h^0_{f,i}(T)$, $s^0_{f,i}(T)$, and $g^0_{f,i}(T)$ trends with temperature but lower $g^0_{f,i}(T)$. This means that for blended systems (oxygen + sulfur), all the oxygenated compounds are thermodynamically more favored, forming CO_x, SO_x, and H_2O, thus reducing the yield to CS_2 and H_2. For this reason, using combined systems or wet charges is not recommended if the final goal is to produce CS_2 and H_2, favoring the H_2S abatement. For the simplified methane reforming, seven compounds are considered in their oxygenated or sulfurized form (*i.e.*, CH_4, C, H_2O/S_2, CO_2/CS_2, CO/CS, H_2O/H_2S, and H_2). Four linearly independent reactions are required to characterize the thermodynamic equilibrium. For this purpose, any combinations from Table 2 can be selected as, for example,

a) *Complete methane reforming* ($\mathbf{R_2}$).
b) Water/H_2S gas shift ($\mathbf{R_5}$).
c) *Complete methane oxidation* ($\mathbf{R_9}$).

https://doi.org/10.1021/acs.energyfuels.3c01237
Energy Fuels XXXX, XXX, XXX−XXX

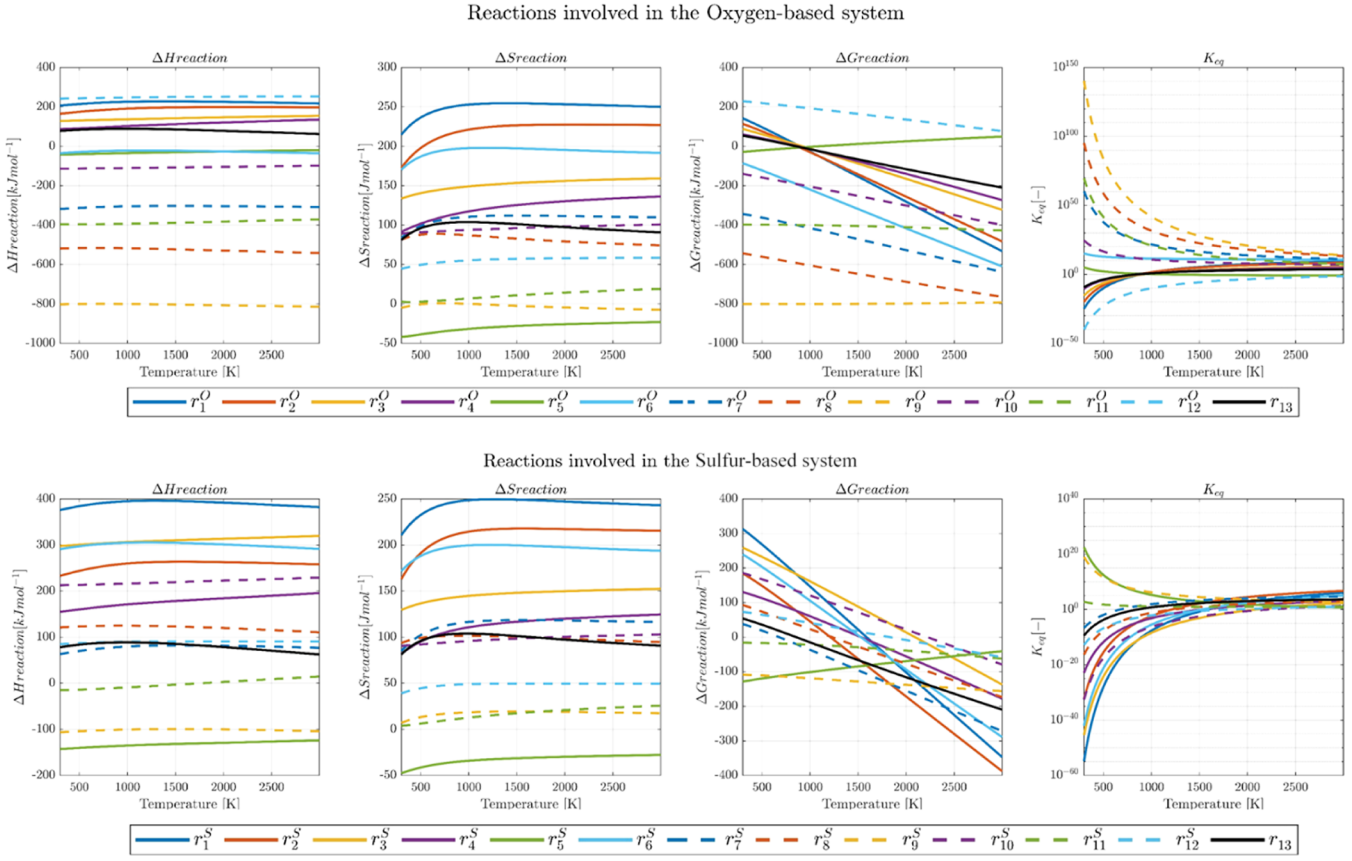

Figure 1. Referring to the reactions in Table 2 $\Delta H^0_{R,j}(T)$, entropy $\Delta s^0_{R,j}(T)$, Gibbs free energy $\Delta h^0_{R,j}(T)$, and $K_{eq,j}(T)$ of reactions in the temperature range 298−3000 K and 1 atm. Top row: reactions with oxygen-based compounds. Bottom row: reactions with sulfur-based compounds.

d) *Methane decomposition* ($\mathbf{R_{13}}$).

Comparing the oxygen-based reaction with the respective sulfur-based reaction, it is possible to observe in Table 2 and Figure 1 that all the oxygen-based reactions have higher $\Delta H^0_{R,j}(T)$ and higher $K_{eq,j}(T)$.

The reactions of complete reforming ($\mathbf{R_2}$) are both (oxygen- and sulfur-based) endothermic. To supply the necessary reaction energy, it is possible to introduce a sub-stoichiometric amount of oxygen (or sulfur) to promote the exothermic reaction of oxidation ($\mathbf{R_9}$). Under these circumstances, it is possible to obtain the overall reaction of partial oxidation ($\mathbf{R_7}$). As it is possible to observe, under this condition, there is no net production or consumption of H_2X, and only for the oxygen case, the overall reaction is exothermic, thus allowing to reach autothermic conditions. Since the reaction enthalpies for $\boldsymbol{R}^S_2$ and $\boldsymbol{R}^S_9$ are, respectively, 232.99 and −106.59 kJ mol^{-1}, to obtain a completely autothermic system, it is necessary to push the oxidation reaction 2.2 times the reforming reaction, leading to an overall production of H_2S and vanishing the possibility of abating its concentration. Since the thermal decomposition of methane occurs under severe conditions, the combustion of coke with sulfur could be an alternative to produce the necessary thermal duty.

The graph displayed in Figure 2 shows that the Gibbs free energy for the reaction $\boldsymbol{R}^S_{11}$ is always negative in the range of temperature examined. This means that the decomposition of CS_2 is always thermodynamically unfavored, while the oxidation of coke with sulfur occurs spontaneously. This is important as it counteracts the formation of carbon from methane decomposition, thus preserving the reactor and the

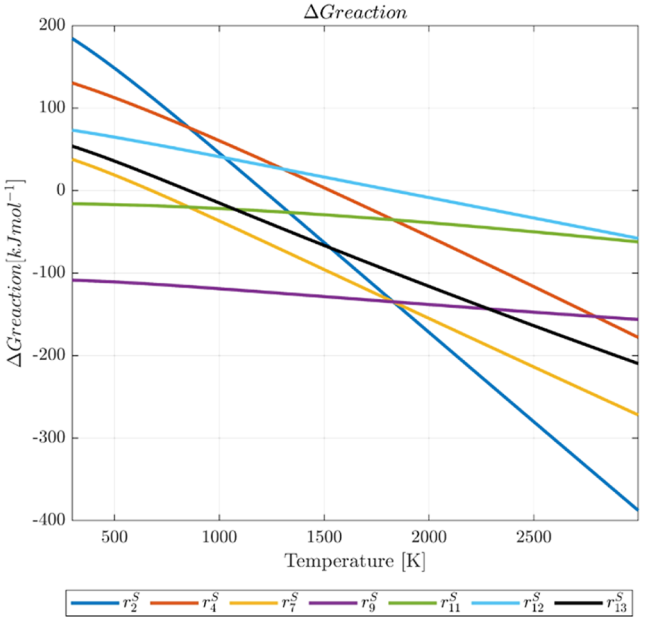

Figure 2. Referring to selected reactions in Table 2, the Gibbs free energy $\Delta G^0_{R,j}(T)$ of reaction in the temperature range 298−3000 K and 1 atm.

catalyst. All the other reactions show a negative slope, meaning that an increase in the reaction temperature shifts the equilibrium toward the products. In this regard, it should be noted that for temperatures lower than 1500 K, the ΔG^0_R

https://doi.org/10.1021/acs.energyfuels.3c01237
Energy Fuels XXXX, XXX, XXX−XXX

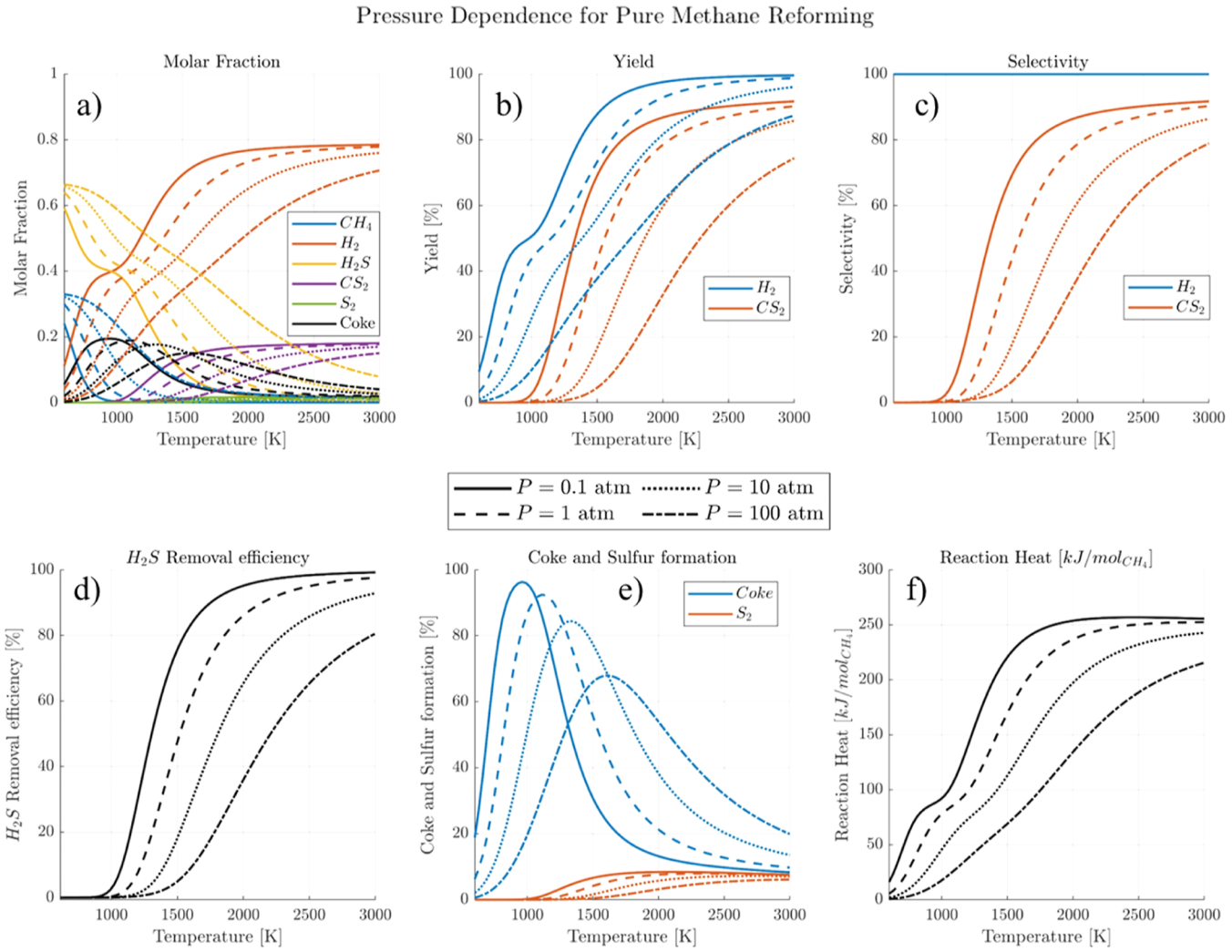

Figure 3. Pressure effect under stoichiometric conditions $\beta = 2$ and $\gamma = 0$. (a) Equilibrium molar fractions; (b) CS_2 and H_2 yields; (c) CS_2 and H_2 selectivities; (d) H_2S removal %; (e) coke and sulfur formation; and (f) reaction heat.

associated with the reforming reaction ($\boldsymbol{R}_2^S$) is higher than that of the methane decomposition ($\boldsymbol{R}_{13}$). Consequently, methane decomposition is favored over the reforming one. For higher temperatures, it is important to notice that the H_2S pyrolysis ($\boldsymbol{R}_{12}^S$) also starts to be thermodynamically favored.

3.2. H_2S–Methane Reforming. After having clarified these preliminary concepts, the thermodynamic equilibria of a reacting gas stream consisting solely of methane (CH_4) and hydrogen sulfide (H_2S) were first investigated by the reaction $\boldsymbol{R}_2^S$. It is worth highlighting that, within the range of temperature and pressure investigated in this work, the methane decomposition reactions $\boldsymbol{R}_{13}$ and the H_2S pyrolysis reactions ($\boldsymbol{R}_{12}^S$) are not negligible. The studied reaction can be performed in a tubular system that is externally heated to enhance the reaction by providing the necessary energy without using partial combustion with oxygen. Considering a system operating under stoichiometric conditions with no additional sulfur (*i.e.*, $\beta = 2$ and $\gamma = 0$), Figure 3 shows the effect of pressure on the thermodynamic equilibrium (simulations at other values of pressure in the range 0.1−100 atm are shown in Figure S3). As it could be expected, an increase in pressure has a negative effect on the reforming reaction, reducing the equilibrium conversion. For this reason, the following considerations are referred to in the case of atmospheric pressure.

The H_2S-reforming reaction starts to be appreciable for temperatures higher than 1000 K, as seen in Figure 3 d, confirming an effective abatement of H_2S in the gas stream. For temperatures higher than 1400 K, the H_2S pyrolysis also starts to become relevant, thus limiting the yield and selectivity to CS_2.

The investigation of the effect of different H_2S/CH_4 (β) in the feed is shown in Figure 4, considering atmospheric pressure and no additional sulfur ($\gamma = 0$).

It is worth considering that with increasing β, the endothermicity of the reaction increases drastically due to the higher amount of H_2S to be converted by the endothermic reforming reaction. Working under sub-stoichiometric conditions, the thermal methane decomposition produces a high amount of coke. By increasing β, the system progressively raises the relative yield to CS_2, which reaches 100% when operating above the stoichiometric conditions. Once the stoichiometric value ($\beta = 2$, circle marker) is exceeded, the methane becomes the limiting reactant, reducing the H_2S removal efficiency and the yield to H_2. At high temperatures, the excess of H_2S thermally decomposes to sulfur that reacts with the coke. A beneficial effect of working with H_2S above

https://doi.org/10.1021/acs.energyfuels.3c01237
Energy Fuels XXXX, XXX, XXX−XXX

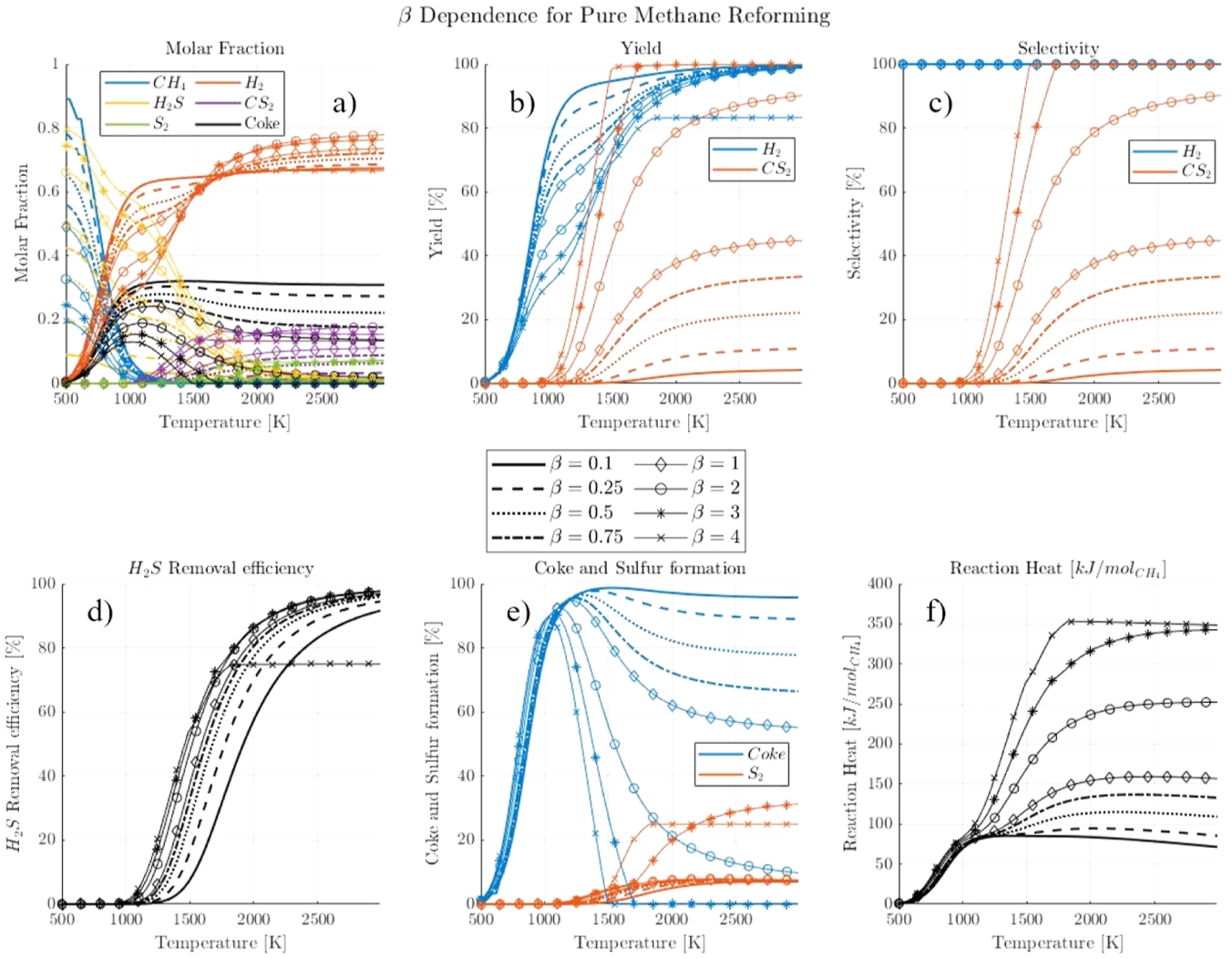

Figure 4. β effect at P = 1 atm and γ = 0. (a) Equilibrium molar fractions; (b) CS_2 and H_2 yields; (c) CS_2 and H_2 selectivities; (d) H_2S removal %; (e) coke and sulfur formation; and (f) reaction heat.

the stoichiometric conditions is the reduction of coke. In fact, observing Figure 4e for high temperatures, there is no coke formation when $\beta > 3$. The coke reacts with the excess of H_2S producing CS_2 and hydrogen, while only the H_2S pyrolysis becomes predominant.

3.3. Sulfur H_2S–Methane Reforming. Several advantages, such as reducing the overall process endothermicity and coke formation, can be obtained by introducing sulfur as the oxidizer. To validate the former point, we first considered the thermodynamic equilibrium of the methane combustion ($\boldsymbol{R}_9^S$) using the sulfur dimer (S_2) as an oxidizer instead of oxygen. As shown in Figure S4, the exothermic reaction tends to be disadvantaged at high temperatures. For this reason, as the ratio $\gamma = \frac{n^0_{S2}}{n^0_{CH4}}$ increases, the influence of temperature impacts the thermodynamic equilibrium more and more (Figure S5). The reaction under consideration ($\boldsymbol{R}_9^S$) was studied in the gaseous state, which explains why there is no substantial influence of pressure as the reaction stoichiometry does not lead to a change in the number of moles.

Assessing the best operative pressure is crucial for the overall process cost. The effect of pressure on the equilibrium composition was studied for a gaseous system under stoichiometric (Figure S6, β = 1 and γ = 0.5) and sub-stoichiometric (Figure S7, β = 0.5 and γ = 0.25) conditions. As observed for the pure H_2S-methane reforming, the increase in pressure plays a negative role in the H_2S conversion at equilibrium. The reforming reaction and the H_2S capture are thermodynamically favored over the combustion reaction with sulfur only at high temperatures (see Figures S6d and S7d). On the other hand, it was observed that working under sub-stoichiometric conditions has the disadvantage of converting less methane into CS_2, thus limiting the yield obtainable, but it allows more effective removal of H_2S even at relatively low temperatures. This phenomenon is due to the competition between the reforming and methane combustion reactions, and the maximum attainable relative yield cannot be 100%. For these reasons, the influence of both parameters γ and β has been studied in the following section considering atmospheric pressure as a reference.

In particular, γ and β were varied in the domain β = [0; 4] and γ = [0; 2], and the effect of the different combinations was studied for different temperatures in the domain [400–2000] K. A complete overview of the obtained results is reported in Figures S8–S16 every 200 K. In Figure 5, the variation of H_2 yield, H_2 selectivity, CS_2 yield, CS_2 selectivity, CH_4 conversion, coke formation, sulfur formation, H_2S removal efficiency, and

https://doi.org/10.1021/acs.energyfuels.3c01237
Energy Fuels XXXX, XXX, XXX–XXX

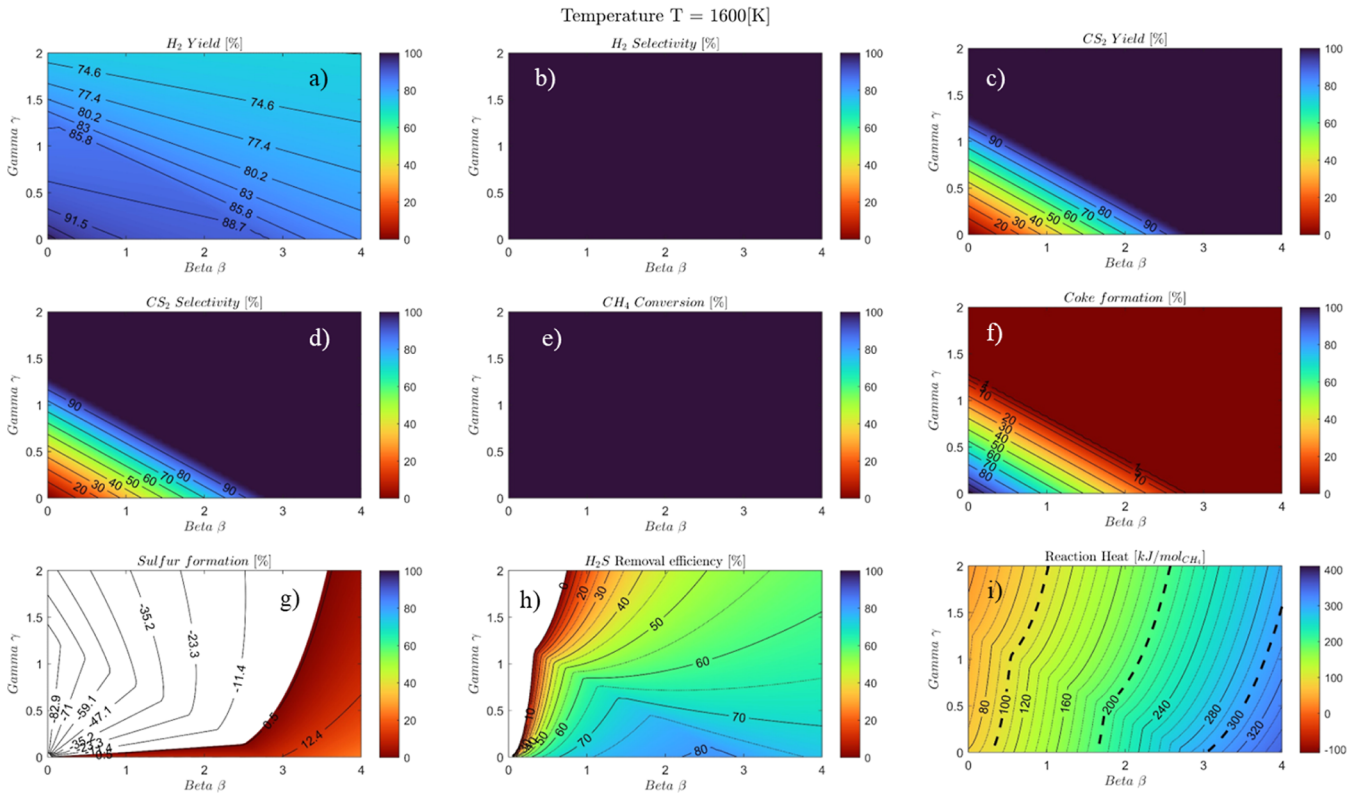

Figure 5. β and γ effect at P = 1 atm and T = 1600 K. (a) H_2 yield [%]; (b) H_2 selectivity [%]; (c) CS_2 yield [%]; (d) CS_2 selectivity [%]; (e) CH_4 conversion [%]; (f) coke formation [%]; (g) sulfur formation [%]; (h) H_2S removal efficiency [%]; and (i) reaction heat [kJ/mol_{CH4}].

reaction heat [kJ/mol_{CH4}] are reported for T = 1600 K, for example.

It is worth considering that in the studied domain, it is possible to highlight two different regions separated by the stoichiometric conditions line ($\beta + 2\gamma = 2$). The influence of β and γ on the different parameters reported in Figure 5 will be discussed individually in the following.

3.3.1. Methane Conversion and Coke Formation. Figure 5f shows the carbon laydown as a function of γ and β (the effect of temperature is visible in Figures S9−S16). Generally, we observe that carbon formation decreases with the increase of both γ and β. The effect of these variables is the result of the greater relative importance of the $\boldsymbol{R}_2^S$ and $\boldsymbol{R}_9^S$ reactions, respectively, which leads to a lower carbon formation. The effect of β agrees with the results presented by other authors,[11] showing a decrease in the threshold temperature for carbon formation (TTC) with the increase of β.

In our case, similarly to what has been reported in the literature, for γ = 0, the minimum value of β for which it is possible to avoid carbon deposition is 3, which corresponds to a TTC of 1700 K. Values of β lower than 3 lead to the formation of carbon, regardless of the temperature. Another important facet highlighted by the data in Figure 6 is the effect of γ on carbon formation. Increasing γ leads to a significant decrease in the threshold temperature for carbon formation. For example, for γ = 0.5 and β = 3, the threshold temperature is 1450 K; a reduction of 250 °C is observed with respect to the case with the same β and γ = 0. The effect of sulfur on the TTC and, more generally, on the lower carbon yields at constant values of β is the consequence of Le Chatêlier's principle for the reaction $\boldsymbol{R}_{11}^S$, which in the range of temperatures examined is strongly shifted toward the

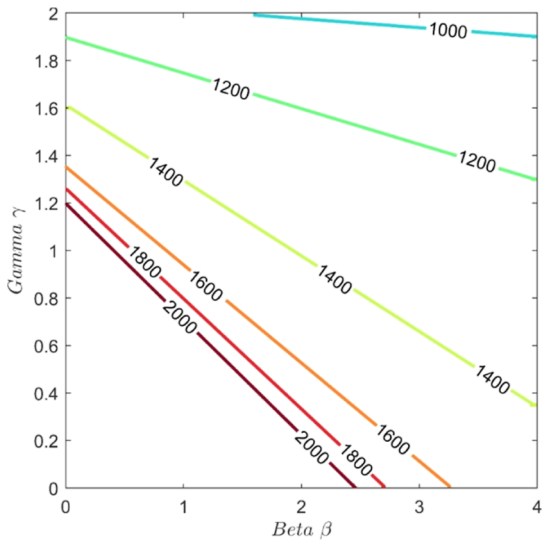

Figure 6. Threshold temperature in [K] for carbon formation.

formation of CS_2. The latter result is significant because it allows the H_2S-SMR reaction to be carried out at lower temperatures without carbon formation, thus making conduction of the process easier and cheaper.

The conditions with no carbon laydown represent optimal operating conditions since the avoidance of solid carbon eliminates problems with either catalyst deactivation or reactor fouling, with a consequent detrimental effect on heat transfer. In this regard, the presence of sulfur in the feed avoids carbon formation at relatively low temperatures and low H_2S/CH_4 ratios. As for the effect of the temperature, increasing values of

https://doi.org/10.1021/acs.energyfuels.3c01237
Energy Fuels XXXX, XXX, XXX−XXX

this parameter lead to a higher presence of reforming and combustion reactions (reactions R_2^S and R_9^S) which in turn counteract carbon formation. The increase in reaction temperature also leads to a higher slope of iso-carbon yields up to γ/β: ~ -0.5, corresponding to a system where equilibrium composition is almost exclusively determined by the reactions R_2^S and R_9^S.

3.3.2. Hydrogen Yields. The data concerning the hydrogen yields are reported in Figure 5a for a temperature of 1600 K and in Figure S17 in the range 400−2000 K. From a general standpoint, the yields of H_2 increase with increasing temperature over the whole range investigated. As pointed out by other authors,[12,18,20] for $\gamma = 0$ (i.e., without feeding sulfur), more than one reaction is responsible for H_2 formation depending on the temperature range. In particular, going from low to high temperatures, methane pyrolysis (R_{13}), reaction of carbon with H_2S, and H_2S pyrolysis (R_{12}^S) occur in the system.

At constant values of β, the increase of γ leads to a decrease in H_2 yields. Keeping in mind the definition of H_2 yields, the inverse relationship between sulfur and H_2 yield results from the reaction between sulfur and methane, yielding CS_2 and H_2S, which depends on the temperature of the system. The decrease in H_2 yields is particularly evident at low temperatures, where the equilibrium of the reforming reaction is still largely shifted to the left.

The increase of both γ and β leads to a lowering of hydrogen yields, which is evident in the whole temperature range investigated. Bearing in mind that the conversion of methane is in any case close to 100%, the inversely proportional relationship between hydrogen yields and β indicates, as already highlighted by other authors[12,18,20] and coherently with the results shown in Figure 2, that the production of hydrogen at low temperatures occurs almost exclusively via methane pyrolysis. A further confirmation is given by the low conversion of H_2S at temperatures lower than 1000 K, while thermodynamic data referring to CH_4 pyrolysis indicate a conversion of 80% at 677 °C, a temperature at which the H_2S conversion is negligible.[24,25] On the other hand, the effect of γ is that of an increased relevance of the reaction R_9^S, which subtracts methane from the reforming reaction, thus leading to a lower yield in H_2.

This effect is particularly evident at a lower temperature where the Gibbs free energy of the reforming reaction has positive or slightly negative values. The temperature increase shifts the overall balance of the reaction toward hydrogen formation, mainly due to the greater importance of the reforming reaction, whose ΔG becomes progressively more negative than that of the competitive reactions. We observed that at 1400 K and $\gamma = 0.5$ and $\beta = 4$, the hydrogen yields are close to 70% without coke formation. As will be shown in the following and can be inferred from the free energy shown in Figure 2, at higher temperatures, a significant fraction of hydrogen derives from the decomposition of H_2S.

3.3.3. H_2S Conversion and Sulfur Yield. Data reported in Figure 5g and in Figure S18 show that up to 800 K, the conversion of H_2S is negligible, indicating that the reforming reaction is still shifted toward the reagents. Higher reaction temperatures lead to lower ΔG of reaction and higher hydrogen yields. H_2S conversion as a function of γ and β shows a complex behavior which is the result of all the reactions involved in the conversion of H_2S. At increasing values of β, we observed a maximum in the H_2S consumption. A similar trend can be observed by closely examining the data referring to H_2S conversion as a function of the H_2S/CH_4 ratio presented by Huang.[12,18] Considering the two reactions involved in the consumption of H_2S, the increase of H_2S conversion for $\beta < 3$ is due to the consideration that H_2S is present in sub-stoichiometric quantities with respect to reactions R_2^S and R_4^S. At higher values, we have an excess of H_2S, which decreases the overall conversion.

The data related to the sulfur yields (see Figure S19) are coherent with the results presented by other authors.[19] In particular, with $\gamma = 0$, above 1000 °C, the pyrolysis of H_2S begins to become meaningful. Compared to the pyrolysis of H_2S alone ($\gamma = 0$; β = infinite), the presence of methane has the effect of reducing the sulfur yield at the same temperature due to the combined effect of the reactions R_2^S and R_9^S and the inverse of the reaction R_{11}^S. Overall, the temperature increase promotes the sulfur yield, which is particularly evident for H_2S/CH_4 ratios higher than the stoichiometric value of the reforming reaction. With the same β, the increase in γ leads to increased sulfur yields for a purely stoichiometric fact. The greater conversion that occurs through the reactions R_2^S and R_9^S is not enough to compensate for the greater quantity of sulfur fed.

3.3.4. Thermal Duty. By using eq 9, it is possible to calculate the heat required to sustain the process. The results at different γ and β are shown in Figure 5i and in Figure S20. It is possible to quantify the percentage of an equivalent amount of methane to burn in order to supply the necessary reaction heat by eq 10, and the results are collected in Figure S21. It is possible to observe the beneficial effect of using sulfur which reduces the necessary thermal duty. It is worth considering that it is possible to distinguish three cases at different temperatures. For temperatures lower than 800 K, the reforming reaction is negligible (see Figure S21), and the combustion of methane (R_9^S) is the predominant reaction that strongly reduces the overall endothermicity caused by the decomposition reactions. In this case, the percentage of burned methane has a maximum value of 10% with respect to the total gas consumed if no sulfur is used. For temperatures between 1000 and 1400 K, the reforming reaction starts to be effective, and increasing β drastically increases the endothermicity. The feeding of sulfur can shift the system to be auto-thermal under certain conditions. For example, at 1200 K, working with $\gamma = 0$; $\beta = 2$, the percentage of burned methane is almost 18% (thermal duty = 145 kJ/mol$_{CH_4}$). Introducing sulfur into the system with $\gamma = 1$; $\beta = 2$, it is possible to reduce the burned methane to 10% (thermal duty = 90 kJ/mol$_{CH_4}$), which corresponds to a saving of 45%, and avoid coke deposition. At higher temperatures, the reforming and pyrolysis reactions start to be predominant, and no appreciable improvements can be observed with the use of sulfur.

3.3.5. Best Operative Conditions. The methane reforming in the presence of H_2S and S has been analyzed from a thermodynamic standpoint. The results showed that using sulfur as a partial feed has several advantages in this process considering the thermal duty, coke deposition, and reaction yield. Since the trends observed in the studied domain are rather complex and involve the interplay of different parameters and responses to take into account, it is possible to define an objective score function to have a simplified process overview. By eq 12, the score is attributed by taking into account (1) the percentage of burned methane, (2) the

https://doi.org/10.1021/acs.energyfuels.3c01237
Energy Fuels XXXX, XXX, XXX−XXX

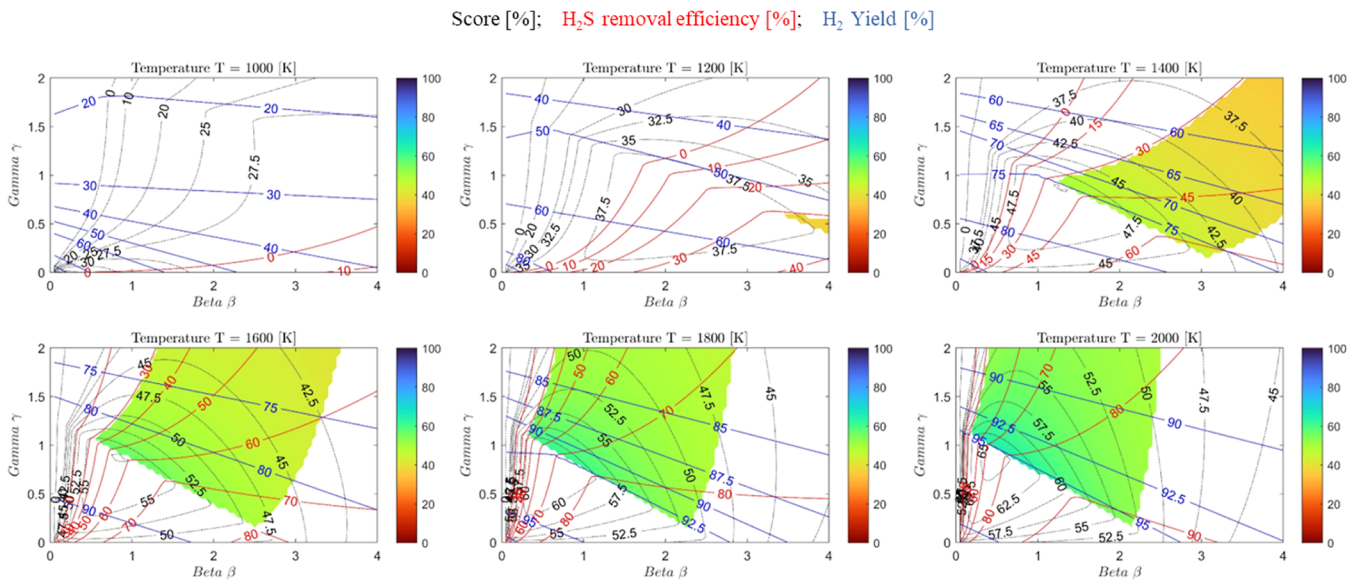

Figure 7. (Dotted black line) Score value [%]; (red line) H_2S removal efficiency [%]; (blue line) hydrogen yield [%] at P = 1 atm, T = 1000÷2000 K in the domain β = [0÷ 4] and γ = [0÷ 2]. Filled domain under the conditions of no coke formation, no sulfur formation, and H_2S removal efficiency > 30%.

net consumption and formation of sulfur, (3) the hydrogen yield, (4) the removal of H_2S, and (5) the methane conversion.

$$\text{SCORE\%} = (-\text{CH}_4^{\text{burned}}\,\% - \partial_{\text{Sulfur}}\,\% + \mu_{\text{H}_2}\,\% + \chi_{\text{H}_2\text{S}}\,\% + \chi_{\text{CH}_4}\,\%)/5 \quad (12)$$

The results in the entire domain are represented in Figure S22. Limiting the domain to the region where there is no coke and sulfur formation and there is an effective H_2S removal higher than 30%, it is possible to observe the results in Figure 7 in the filled part of the domain. It is worth considering that the best score value increases with the temperature and is located in the region near γ = 1.2; β = 0.5 with an H_2 yield of 90% and a H_2S removal of 50% at 1800 K. Operating at the same temperature, with γ = 0.7; β = 1, it is possible to increase the H_2S removal up to 80% with a significant reduction of the score function due to the increase in the process endothermicity.

Following these considerations, we can conclude that the best operative conditions need to be assessed based on a detailed process plant economic evaluation due to the high number of factors and contributions to take into account.

4. CONCLUSIONS

The sulfur-H_2SMR is the only possible way to produce hydrogen from the H_2S methane reforming without producing carbon and sulfur deposits and having an effective H_2S removal from the gas stream. Using sulfur to enhance the H_2SMR has several advantages from the thermodynamic analysis. In fact, it can reduce the thermal duty required by such an endothermic reaction and hinder the coke formation, which is extremely important to prevent fouling of the reactor and of the catalyst, which could lead to premature shutdowns of an industrial plant. Despite these advantages, several key aspects still need to be explored since the operative temperature is very high, and the presence of these compounds is hazardous for toxicity, corrosion, and flammability risks. Future development could focus on using gas streams with higher carbon sources to promote the sulfur extraction capacity from the H_2S fraction and using inert gas to shift and increase the conversion to lower operative temperatures.

■ ASSOCIATED CONTENT

Supporting Information

The Supporting Information is available free of charge at https://pubs.acs.org/doi/10.1021/acs.energyfuels.3c01237.

Additional thermodynamic equations, data of CH_4 conversion, H_2 yield and selectivity, CS_2 yield and selectivity, coke formation, sulfur formation, and H_2S conversion at different temperatures in the investigated domain (PDF)

■ AUTHOR INFORMATION

Corresponding Author

Davide Moscatelli − *Department of Chemistry, Materials, and Chemical Engineering "Giulio Natta", Politecnico di Milano, Milan 20133, Italy;* orcid.org/0000-0003-2759-9781; Email: davide.moscatelli@polimi.it

Authors

Flavio Tollini − *Department of Chemistry, Materials, and Chemical Engineering "Giulio Natta", Politecnico di Milano, Milan 20133, Italy*

Mattia Sponchioni − *Department of Chemistry, Materials, and Chemical Engineering "Giulio Natta", Politecnico di Milano, Milan 20133, Italy;* orcid.org/0000-0002-8130-6495

Vincenzo Calemma − *Research and Technological Innovation Department, ENI SPA, San Donato Milanese 20097, Italy*

Complete contact information is available at: https://pubs.acs.org/10.1021/acs.energyfuels.3c01237

Author Contributions

Conceptualization: F.T., V.C.; data curation: F.T.; investigation: F.T.; supervision: D.M., M.S.; funding acquisition: D.M., V.C.; writing—original draft: F.T., V.C.; writing—

https://doi.org/10.1021/acs.energyfuels.3c01237
Energy Fuels XXXX, XXX, XXX−XXX

review and editing: F.T., V.C., M.S. All authors have read and given approval to the final version of the manuscript.

Notes

The authors declare no competing financial interest.

■ ACKNOWLEDGMENTS

The authors express their gratitude to Eni S.p.A. for the financial support.

■ SYMBOLS

CO_2 = carbon dioxide
CS_2 = carbon disulfide
CG = coal gasification
EoS = equation of state
GHGs = greenhouse gases
H_2SMR = H_2S methane reforming
H_2 = hydrogen
H_2S = hydrogen sulfide
IEA = International Energy Agency
CH_4 = methane
NR = number of reactions
OG = oil gasification
SRK = Soave−Redlich−Kwong
SMR = steam methane reforming
$S-H_2SMR$ = sulfur H_2S methane reforming
TTC = threshold temperature for the carbon formation

■ ABBREVIATIONS AND ACRONYMS

a_i = activity of the i-th compound
P = pressure
χ_i = conversion of the i-th compound
∂_i = deposition of the i-th compound
$K_{eq,j}(T)$ = equilibrium constant the generic j-th
λ_j = extent of the generic j-th reaction
$C^0_{p,i}(T)$ = heat capacity of the i-th compound
ΔH_i^{comb} = heat of combustion of the i-th compound
mol_i^{in} = inlet molar rate of the i-th compound
β = inlet molar ration of H_2S/CH_4
γ = inlet molar ration of S_2/CH_4
$h^0_{f,i}(T)$ = molar enthalpy of formation of the i-th compound
$\Delta h^0_{R,j}(T)$ = molar enthalpy of the generic j-th reaction
$s^0_{f,i}(T)$ = molar entropy of formation of the i-th compound
$\Delta s^0_{R,j}(T)$ = molar entropy of the generic j-th reaction
$g^0_{f,i}$ = molar Gibbs free energy of formation of the i-th compound
$\Delta h^0_{R,j}(T)$ = molar Gibbs free energy of the generic j-th reaction
$mol_{CH_4}^{burned}$ = moles of burned methane
$mol_{CH_4}^{reformed}$ = moles of reformed methane
mol_i^{out} = outlet molar rate of the i-th compound at thermodynamic equilibrium
CH_4^{burned} % = percentage of burned methane respect the total (reformed + burned)
R_i^O = *reaction oxygen-based*
R_i^S = *reaction sulfur-based*
σ_i = selectivity of the i-th compound
$\nu_{i,j}$ = stoichiometric vector of the generic reaction j-th of the compounds i-th
T = temperature
Q = thermal duty
R = universal gas constant
μ_i = yield of the i-th compound

■ REFERENCES

(1) T-Raissi, A. *Hydrogen from Renewable Power: Technology Outlook for the Energy Transition*, 2018. www.irena.org.
(2) *IEA for the G20, J. The Future of Hydrogen. The Future of Hydrogen*. https://www.iea.org/reports/the-future-of-hydrogen, 2019.
(3) Leprince, P. Conversion Processes. In *Conversion Processes*; Edition Technip, 2001.
(4) Spath, P. L.; Mann, M. K. *Life Cycle Assessment of Hydrogen Production via Natural Gas Steam Reforming*, 2003;. https://www.nrel.gov/docs/fy01osti/27637.pdf.
(5) Bhandari, R.; Trudewind, C. A.; Zap, P. *Life Cycle Assessment of Hydrogen Production Methods-A Review*; Institut für Energie und Klimaforschung, 2012.
(6) Dou, B.; Wu, K.; Zhang, H.; Chen, B.; Chen, H.; Xu, Y. Sorption-enhanced chemical looping steam reforming of glycerol with CO2 in-situ capture and utilization. *Chem. Eng. J.* **2023**, *452*, 139703.
(7) IEA. *World Energy Outlook, Natural Gas Resources and Production Prospects*, 2008.
(8) Global sulfur production worldwide in 2020, by country. https://www.statista.com/statistics/1031181/sulfur (accessed January 17, 2023).
(9) Speight, J. G. *Natural Gas: A Basic Handbook*; Gulf Professional Publishing, 2019; p 277.
(10) Reverberi, A. pietro; Klemeš, J. J.; Varbanov, P. S.; Fabiano, B. A review on hydrogen production from hydrogen sulphide by chemical and photochemical methods. *J. Clean. Prod.* **2016**, *136*, 72−80.
(11) de Crisci, A. G.; Moniri, A.; Xu, Y. Hydrogen from hydrogen sulfide: towards a more sustainable hydrogen economy. *Int. J. Hydrogen Energy* **2019**, *44*, 1299−1327.
(12) Huang, C.; T-Raissi, A. Liquid hydrogen production via hydrogen sulfide methane reformation. *J. Power Sources* **2008**, *175*, 464−472.
(13) El-Melih, A. M.; al Shoaibi, A.; Gupta, A. K. Hydrogen sulfide reformation in the presence of methane. *Appl. Energy* **2016**, *178*, 609−615.
(14) El-Melih, A. M.; Iovine, L.; al Shoaibi, A.; Gupta, A. K. Production of hydrogen from hydrogen sulfide in presence of methane. *Int. J. Hydrogen Energy* **2017**, *42*, 4764−4773.
(15) Li, Y.; Yu, X.; Guo, Q.; Dai, Z.; Yu, G.; Wang, F. Kinetic study of decomposition of H2S and CH4 for H2 production using detailed mechanism. *Energy Procedia* **2017**, *142*, 1065−1070.
(16) Li, Y.; Yu, X.; Li, H.; Guo, Q.; Dai, Z.; Yu, G.; Wang, F. Detailed kinetic modeling of homogeneous H2S-CH4 oxidation under ultra-rich condition for H2 production. *Appl. Energy* **2017**, *208*, 905−919.
(17) Megalofonos, S. K.; Papayannakos, N. G. Hydrogen production from natural gas and hydrogen sulphide. *Int. J. Hydrogen Energy* **1991**, *16*, 319−327.
(18) Huang, C.; T-Raissi, A. Thermodynamic analyses of hydrogen production from sub-quality natural gas: Part II: Steam reforming and autothermal steam reforming. *J. Power Sources* **2007**, *163*, 637−644.
(19) Spatolisano, E.; De Guido, G.; Pellegrini, L. A.; Calemma, V.; de Angelis, A. R.; Nali, M. Process sensitivity analysis and techno-economic assessment of hydrogen sulphide to hydrogen via H2S methane reformation. *J. Clean. Prod.* **2022**, *330*, 129889.
(20) Spatolisano, E.; De Guido, G.; Pellegrini, L. A.; Calemma, V.; de Angelis, A. R.; Nali, M. Hydrogen sulphide to hydrogen via H2S methane reformation: Thermodynamics and process scheme assessment. *Int. J. Hydrogen Energy* **2022**, *47*, 15612−15623.
(21) Database, N. S. R. *NIST Chemistry WebBook*, 2023. https://webbook.nist.gov/chemistry/.
(22) Green, D. W.; Perry, R. H. *Perry's Chemical Engineers' Handbook*; McGraw-Hill Education, 2008.
(23) Shomate, C. H. A method for evaluating and correlating thermodynamic da ta. *J. Phys. Chem.* **1954**, *58*, 368−372.

https://doi.org/10.1021/acs.energyfuels.3c01237
Energy Fuels XXXX, XXX, XXX−XXX

(24) Marquardt, T.; Bode, A.; Kabelac, S. Hydrogen production by methane decomposition: Analysis of thermodynamic carbon properties and process evaluation. *Energy Convers. Manag.* **2020**, *221*, 113125.
(25) Leal Pérez, B. J.; Medrano Jiménez, J. A.; Bhardwaj, R.; Goetheer, E.; van Sint Annaland, M.; Gallucci, F. Methane pyrolysis in a molten gallium bubble column reactor for sustainable hydrogen production: Proof of concept & techno-economic assessment. *Int. J. Hydrogen Energy* **2021**, *46*, 4917−4935.

https://doi.org/10.1021/acs.energyfuels.3c01237
Energy Fuels XXXX, XXX, XXX−XXX